

Preference-Based Whale Optimization Algorithm for Multi-Objective Structural Optimization Problems Using Reference Points

Dênis E. C. Vargas¹, Afonso C. C. Lemonge², Elizabeth F. Wanner³

¹*Dept. of Mathematics, Federal Center for Technological Education of Minas Gerais - CEFET-MG
Belo Horizonte, Brazil*

denis.vargas@cefetmg.br

²*Dept. of Applied and Computational Mechanics, Faculty of Engineering, Federal University of Juiz de Fora - UFJF, Juiz de Fora, Brazil*

afonso.lemonge@ufff.br

³*Dept. of Computer Engineering, Federal Center for Technological Education of Minas Gerais - CEFET-MG
Belo Horizonte, Brazil*

efwanner@cefetmg.br

Abstract. Several structural optimization problems can be formulated as multi-objective optimization problems (MOOPs) due to the existence of multiple conflicting objectives, which must be minimized simultaneously. Most MOOP solvers find the Pareto front formed by the best trade-off solutions, and then the decision-maker (DM) chooses the one that best meets his/her personal preferences. However, many Pareto front solutions have no chance of being chosen once they are outside DM's region of interest (ROI). On the other hand, some solvers use information from the DM's preferences and can focus only on DM's ROI rather than all Pareto front, consequently obtaining better solutions from the DM's perspective. This work proposes an algorithm named R-WOA to solve the multi-objective structural optimization problems (MOSOPs) using the Whale Optimization Algorithm (WOA) guided by reference points formed by DM's desired values for the objective functions. MOSOPs having 10-, 25-, 60-, 72-, and 942-bar trusses are carried out to test the R-WOA's performance. The numerical experiments compare the R-WOA with algorithms R-NSGA-II, R-GDE3, and R-GDE3+APM regarding Hypervolume and IGD+ performance measures. Using a non-parametric statistical test and the Performance Profile, the R-WOA proves to be competitive in most of test scenarios.

Keywords: Multi-objective structural optimization problem, Whale optimization algorithm, Reference point

1 Introduction

Real-world engineering problems frequently demand simultaneous optimization of multiple conflicting objective functions. Mathematically, these problems can be described as multi-objective optimization problems (MOOPs), whose goal is to find the solutions that represent the best trade-offs between all objectives. Those solutions are called Pareto optimal ones.

Concerning the design of structures, minimum cost, optimal safety performance, environmental conditions, and serviceability are set as criteria and/or constraints in the so called multi-objective structural optimization problems (MOSOPs). A widespread kind of MOSOP involves truss structures, in which a decision-maker (DM) wants to minimize the entire structure's weight and the maximum nodal displacement of the bars, constraining the stress subjected to each bar to a maximum value to ensure the final design's safety.

Multi-Objective Evolutionary Algorithms (MOEAs) are the most common approaches used in solving a MOOP, mainly because they can obtain a set of Pareto optimal solutions in a single run. There are several studies in which MOEAs are used to solve MOSOPs concerning truss structures in the literature, as shown in [1].

Most MOEAs find the Pareto front formed by the image, in the objective function space, of all obtained Pareto optimal solutions. Then the DM picks the one that best satisfies his/her personal choices. But since many Pareto front solutions are outside the DM's region of interest (ROI), they have no chance of being chosen. In these cases, MOEAs using the DM's preference information have the advantage of avoiding undesired solutions and deepening the search into DM's ROI, getting better solutions from the DM's point of view.

In [2], *a priori* reference based-MOEAs was used in which the reference points represented the DM's desired values for the objective functions to solve MOSOPs. The performance of three MOEAs was assessed: the well-known Reference Point NSGA-II (R-NSGA-II), the Third Evolution Step of Generalized Differential Evolution (GDE3) guided by reference points in the same way that R-NSGA-II (dubbed R-GDE3), and the R-GDE3+APM, the R-GDE3 equipped with the constraint-handling technique called Adaptive Penalty Method (APM). These algorithms were used to solve MOSOPs concerning 10-, 25-, 60-, 72-, and 942-bar trusses.

Inspired by the hunting' method of humpback whales, which creates bubbles diving and rising surrounding their prey in a spiral shape, [3] proposed the Whale Optimization Algorithm (WOA). Basically, the algorithm works with three actions named encircling prey (whales identify the prey's location and encircle them), spiral bubble-net feeding maneuver (exploitation phase), and search for prey (exploration phase). Despite several studies using WOA to solve MOOPs can be found in the literature, no work using DM's preference information in a WOA-based MOEA search process was found to the best of our knowledge.

It is worthwhile to mention that, in the seminal paper [3], the authors applied WOA for solving a single-objective formulation for the structural optimization design problems of the 15-, 25-, and 52-bar trusses. For the 15-bar truss problem, WOA found an identical structure compared to the other evaluated algorithms with the second smallest number of function evaluations. For the 25-bar truss problem, WOA obtained the best weight than the algorithms considered. For the 52-bar truss problem, WOA found the best weight with the smallest number of function evaluations compared to other evaluated algorithms. Motivated by the competitive results on these single-objective problems, we aim to explore its capabilities when solving MOSOPs when DM's preference information is available.

This paper proposes the R-WOA, a WOA-based MOEA using reference points in the same way as R-NSGA-II. R-WOA to solve the same set of MOSOPs as in [2]. The problem set comprises the continuous case concerning the 10-, and 25-bar trusses, and the both discrete and continuous cases of the 60-, 72-, and 942-bar trusses. The R-WOA, R-GDE3+APM, R-GDE3, and R-NSGA-II are used to solve the problems for comparison purposes.

The remainder of the paper is organized as follows. Section 2 defines the MOSOPs adopted here. Section 3 presents the WOA and describes the proposed R-WOA algorithm. Section 4 shows the computational experiments: the parameter setting, the performance measures, and an analysis of the results. Finally, Section 5 presents the conclusions and future work.

2 Multi-Objective Structural Problem Formulation

The proposed MOSOP consists in obtaining a set of design variables $\mathbf{x} = (x_1, \dots, x_n)$ that represents the bar's cross-sectional areas of the trusses (A_1, \dots, A_n) , minimizing the total weight of the structure along with the maximum displacement of its nodes. To ensure the safety of the final design, the stress on each bar cannot exceed a specific maximum limit. Mathematically, the problem is formulated as:

$$\begin{aligned} \min \quad & f_1(\mathbf{x}) = \sum_{i=1}^n \rho A_i L_i \quad \text{and} \quad \min f_2(\mathbf{x}) = \max(|u_{jl}|) \\ \text{s.t.} \quad & |s_{il}| \leq s_{adm} \\ & j = 1, \dots, M \quad l = 1, \dots, N_L \end{aligned} \quad (1)$$

in which $s_{il}(\mathbf{x}) = E\varepsilon_{il}(\mathbf{u}(\mathbf{x}))$ are the limits of the normal stress (constraints), E is the Young's modulus, n is the total number of bars in the truss structure, M is the number of degrees of freedom, N_L is the number of load cases applied to the structure, L_i is the length of the i -th bar, ρ is the density of the material, u_{jl} is the nodal displacement of the j -th degree of freedom, s_{il} is the normal stress of the i -th bar, all in the l -th load case, s_{adm} is the allowed normal stress, and $\varepsilon_{il}(\mathbf{u}(\mathbf{x}))$ is the normal strain in the axial direction of the bar. When the design variables are discrete, the vector $\mathbf{x} = (x_1, \dots, x_n)$ refers to the cross-sectional areas of the bars (A_1, \dots, A_n) in the following way: the i -th cross-sectional area is $A_{[x_i]}$, in which $[x_i] = \text{round}(x_i)$ is an index for elements of the set of possible values $AP = \{A_1, \dots, A_{|AP|}\}$, $|AP|$ is the total number of elements in AP , $1 \leq x_i \leq |AP|$, $i = 1, \dots, n$. In the continuous case, $A_i = x_i$, $\underline{x}_i \leq x_i \leq \bar{x}_i$, in which $\underline{\mathbf{x}} = (\underline{x}_1, \dots, \underline{x}_n)$ and $\bar{\mathbf{x}} = (\bar{x}_1, \dots, \bar{x}_n)$ are the lower and upper bounds of the cross-sectional areas, respectively.

3 Whale Optimization Algorithm (WOA)

Whale Optimization Algorithm (WOA), proposed in [3], mimics the hunting mechanism of humpback whales in nature. In WOA, the whales are search agents which work based on three actions: encircling prey, spiral bubble-

net feeding maneuver, and search for prey. In the encircling prey action, whales consider the current best search agent as a target prey and update their positions encircling it. Let $\vec{X}(t)$ be a search agent in current iteration t , and $\vec{X}^*(t)$ the current best search agent so far. The equations related to this action are given by:

$$\vec{D} = |\vec{C} \cdot \vec{X}^*(t) - \vec{X}(t)| \quad \text{and} \quad \vec{X}(t+1) = \vec{X}^*(t) - \vec{A} \cdot \vec{D} \quad (2)$$

in which

$$\vec{A} = 2\vec{a} \cdot \vec{r} - \vec{a} \quad \text{and} \quad \vec{C} = 2\vec{r} \quad (3)$$

with all \vec{a} components equal to $2 - 2t/t_{max}$ and \vec{r} is a random vector with components in $[0, 1]$.

The spiral bubble-net feeding maneuver action represents the exploitation phase and simulates the behavior of an attack method in the form of a spiral trajectory. The equations associated with this action are given by:

$$\vec{X}(t+1) = |\vec{X}^*(t) - \vec{X}(t)|e^{bl} \cos(2\pi l) + \vec{X}^*(t) \quad (4)$$

in which b is a parameter that determines the logarithmic spiral's shape and $-1 \leq l \leq 1$ is a random number.

The search for prey action represents the exploration phase, in which the search agents update their positions randomly according to the position of each other. The equations associated are the same as Equation (2), replacing \vec{X}^* by \vec{X}_{rand} .

WOA assumes a probability of 50% to update the position of whales by spiral bubble-net feeding maneuver, controlled by a random variable $p \in [0, 1]$. So, Equation (4) is used if $p \geq 0.5$. Otherwise, one of the actions, encircling prey or search for prey, is selected according to the value of $|\vec{A}|$ to control the exploration phase. At the beginning of the search process, the value of $|\vec{A}|$ has more chances to be greater than or equal to 1. Thus, if $|\vec{A}| \geq 1$ then search for prey action is selected. Otherwise, search agents update their positions with encircling prey action. More details about WOA can be found at [3].

3.1 R-WOA

The proposed algorithm, dubbed R-WOA, uses the same design as R-NSGA-II [4]. Parent and offspring populations in R-NSGA-II are merged, and the solutions with the best ranks are chosen. The main difference between R-NSGA-II and NSGA-II is the crowding distance notion.

Different from the original concept of crowding distance in NSGA-II [5], which aims to spread solutions over all the Pareto front, a modified crowding distance is proposed in R-NSGA-II: the weighted normalized Euclidean distance for each reference point $\vec{z} = (z_1, \dots, z_m)$ of each solution \mathbf{x} :

$$d_{\mathbf{x}, \vec{z}} = \sqrt{\sum_{k=1}^m w_k \left(\frac{f_k(\mathbf{x}) - \vec{z}_k}{f_k^{MAX} - f_k^{MIN}} \right)^2} \quad (5)$$

in which f_k^{MAX} and f_k^{MIN} are the maximum and minimum values, respectively, of k -th objective function, $k = 1, \dots, m$, and $w_k = 1/m$ by default. The nearest solutions to all reference points are preferred, while a user-defined parameter ϵ controls the diversity of the population around the reference points. In [4], the authors implemented the R-NSGA-II using the simulated binary crossover (SBX).

R-WOA is a WOA-based MOEA that uses reference points in the same way as R-NSGA-II, in which the WOA replaces the SBX crossover. The algorithm randomly selects a feasible non-dominated solution in the current iteration t as the best search agent $\vec{X}^*(t)$. Moreover, R-WOA has a crossover rate (CR) to decide whether or not to update the j th search agent's position, in addition to having an external file storing the non-dominated solutions discovered during its execution.

4 Numerical Experiments

The proposed R-WOA is employed to solve the MOSOP of the Equation 1. We use 8 different test scenarios: MOSOPs concerning 10-, 25-bar trusses (continuous case), and 60-, 72-, and 942-bar trusses (both discrete and

continuous cases). The problems are the same as the ones shown in [2]. A complete definition of these MOSOPs can be seen in [6].

To assess the performance of R-WOA, R-NSGA-II, R-GDE3, and R-GDE3+APM are used as a comparison since they were used in [2] to solve exactly the same problems. Thirty independent runs of all algorithms have been performed with a population of 50 search agents during 1000 iterations. Performance measures such as Hypervolume [7] and IGD+ [8] are employed to evaluate the non-dominated fronts of the algorithms regarding convergence and distribution. These performance measures have been calculated considering solutions belonging to the DM's ROI for each problem (the same as [2]).

A non-parametric statistical test is used to assess whether there is a difference in performance in the results or not. In [2], the authors compared the performance among the R-NSGA-II, R-GDE3, and R-GDE3+APM in an *all-versus-all* approach. Here, we aim to compare the non-dominated solutions in an *all-versus-one* approach. The Wilcoxon Rank Sum Test is used to verify whether two samples are likely to come from the same population. Using 0.05 as the significance level, the statistical test is defined as:

$$\begin{cases} H_0 = \mu_{R-WOA} - \mu_i = 0 \\ H_1 = \mu_{R-WOA} - \mu_i \neq 0 \end{cases} \quad (6)$$

in which μ_{R-WOA} represents the median from all runs for R-WOA and μ_i represents the median from all runs for R-NSGA-II, R-GDE3, and R-GDE3+APM. Observe that the Wilcoxon Rank Sum Test is performed as a two-sided test and, if the null hypothesis is rejected, we can only say the two algorithms are not equal but not specify directionality. In this way, a pos-hoc test is applied to identify where the difference lies.

The R-WOA parameters are $\epsilon = 0.001$ for 10-, 25-, and 72-bar trusses (continuous case), $\epsilon = 0.005$ for 60-, and 72-bar trusses (discrete case) and 942-bar trusses (both discrete and continuous cases), and $\epsilon = 0.01$ for 60-bar truss (continuous case). Except for 60-bar trusses (both discrete and continuous cases), in which $CR = 0.1$, the crossover rate for all other problems was $CR = 1$. These parameters have been chosen based on the results during a preliminary experiment. In addition, the WOA parameter b has been set as 1 for all MOSOPs. The parameters for R-NSGA-II, R-GDE3, and R-GDE3+APM have been set as described in [2].

Aiming to visualize and to better interpret the results of Hypervolume and IGD+, Performance Profiles [9] have been employed. The Performance profile provides a graphical representation of the distribution of performance measures over a given problem set taking into account the number of problems solved and the cost (calculated here as the performance measure) it took to solve it. Let P be a set of n_p problems, S a set of algorithms, and $t_{p,s}$ any performance measure evaluated in problem p by algorithm s . We define the performance ratio as

$$r_{p,s} = \frac{t_{p,s}}{\min\{t_{p,s}, s \in S\}}.$$

The Performance Profile $\rho_s(\tau)$ is then defined as the probability that the performance ratio $r_{p,s}$ of algorithm $s \in S$ is within a factor $\tau \geq 1$ of the best possible ratio. In other words, the performance profile is given by:

$$\rho_s(\tau) = \frac{1}{n_p} |\{p \in P : r_{p,s} \leq \tau\}|.$$

Considering an algorithm s and each value of a positive factor τ , the Performance Profile represents the percentage of problems extracted from P on which the performance of s is within a factor of τ of the best performance of other algorithms. Although the Performance Profiles have been originally proposed to compare deterministic optimization algorithms, in [10] the authors have demonstrated that the area below $\rho_s(\tau)$ can be used as an overall performance measures of a given stochastic algorithm s .

4.1 Results

The mean and standard deviation of the Hypervolume and IGD+ values for the Pareto front concerning algorithms R-WOA, R-NSGA-II, R-GDE3, and R-GDE3+APM are displayed in Table 1. The (+) indicates if there is a statistical difference between R-WOA and the corresponding algorithm and the algorithm with superior performance is displayed in bold. Figures 1a and 1b show the Performance Profiles of these table results, jointly with the areas under the curves (proportionally to the biggest) for Hypervolume and IGD+, respectively. These profiles can help us visualize the R-WOA overall performance taking into account all test problems and the considered performance measures.

Considering the Hypervolume in Table 1, R-WOA has outperformed its competitors in all test problems except when compared to R-NSGA-II in problems having 10- and 60-bar trusses (discrete case). In those test

scenarios, it is not possible to say there is a difference between R-WOA and R-NSGA-II. When assessing the algorithms' performance over all problems, the R-WOA has achieved the best performance regarding to Hypervolume indicator (Figure 1a). The higher under the curve value for R-WOA corroborates the results presented in Table 1 showing a superiority of R-WOA when Hypervolume is employed.

Considering the IGD+ in Table 1, there is no statistical difference between pairs of algorithms in problem having 10-bar trusses. In problem having 72-bar trusses (continuous case), there only is a statistical difference favouring R-NSGA-II over R-WOA. In problem having 942-bar trusses (both continuous and discrete case), although R-WOA outperforms R-GDE3 and R-GDE3+APM, it is outperformed by R-NSGA-II. Once again, when assessing the algorithms' performance over all problems, R-WOA has achieved the second-best performance concerning IGD+ (Figure 1b). Even though the Performance Profile indicates a superiority favouring R-NSGA-II when using IGD+, the difference between R-NSGA-II and R-WOA is subtle.

Figures 2a-2h shows the combined Pareto front obtained in 30 independent runs for all MOSOPs. Some regions of the Pareto front are enlarged to analyze the behaviors of the algorithms. As pointed out in [2], R-NSGA-II uses SBX operator which tends to create offspring near the parents, generating Pareto optimal solutions much closer to the reference point than those achieved by the other MOEAs in some MOSOPs (Figures 2a, 2g, and 2h). This may have favoured the good result obtained in the Performance Profile regarding the IGD+ indicator. On the other hand, R-WOA obtained a better distributed Pareto front in the ROI for some MOSOPs, dominating solutions at least one of the extremities and favoring its good Hypervolume values (Figures 2a, 2b, 2c, 2e, 2g, and 2h).

In the 60-bar truss MOSOP (continuous case), the solutions obtained by R-WOA dominate solutions at the middle of the Pareto front and are nearer to the reference point when compared to those attained by the other MOEAs. In this case, R-WOA achieved the best performance regarding both Hypervolume and IGD+ indicators, with statistically significant differences in all the scenarios.

Table 1. Means (M) and Standard Deviations (SD) of Hypervolume and IGD+ values: (c) and (d) correspond to the continuous and discrete cases, respectively. (+) indicate p-values < 0.05 (Wilcoxon Rank Sum Test) regarding the R-WOA. The indicator value of the superior algorithm is in bold. The values in the first column indicate the number of truss bars.

Problem		Hypervolume				IGD+			
		R-WOA	R-NSGA-II	R-GDE3	R-GDE3+APM	R-WOA	R-NSGA-II	R-GDE3	R-GDE3+APM
10c	M	0.84646	0.83886	0.73980(+)	0.75482(+)	0.00842	0.00359	0.08808	0.07493
	SD	0.00431	0.01158	0.17342	0.16370	0.00423	0.00421	0.15901	0.15568
25c	M	0.67872	0.67236(+)	0.61651(+)	0.62431(+)	0.00037	0.00051(+)	0.03273(+)	0.02704(+)
	SD	0.00068	0.00365	0.06721	0.05903	0.00014	0.00017	0.05680	0.04888
60c	M	0.74742	0.72966(+)	0.73080(+)	0.72861(+)	0.00633	0.01170(+)	0.02787(+)	0.03071(+)
	SD	0.00362	0.01095	0.01393	0.02079	0.00565	0.00396	0.02114	0.02448
60d	M	0.65461	0.65751	0.63398(+)	0.63919(+)	0.01361	0.01367(+)	0.02715(+)	0.02354(+)
	SD	0.02293	0.00725	0.04367	0.03709	0.01504	0.00451	0.03158	0.02685
72c	M	0.70939	0.70561(+)	0.67282(+)	0.67703(+)	0.00931	0.00144(+)	0.01653	0.01457
	SD	0.01834	0.00644	0.04619	0.02803	0.01225	0.00037	0.03382	0.02166
72d	M	0.64170	0.63566(+)	0.62632(+)	0.62362(+)	0.00106	0.00451(+)	0.01120(+)	0.01327(+)
	SD	0.00242	0.00267	0.00509	0.01552	0.00171	0.00177	0.00348	0.01088
942c	M	0.87336	0.86616(+)	0.82973(+)	0.82346(+)	0.01744	0.01482(+)	0.03942(+)	0.04411(+)
	SD	0.00844	0.00500	0.03941	0.04594	0.00490	0.00438	0.02741	0.03183
942d	M	0.87426	0.86751(+)	0.83252(+)	0.84429(+)	0.01934	0.01625(+)	0.03488(+)	0.02777(+)
	SD	0.00484	0.00586	0.03063	0.02336	0.00407	0.00361	0.02012	0.01541

5 Conclusion

This paper proposed an approach to solve multi-objective structural optimization problems (MOSOPs). The algorithm, named R-WOA, combined the Whale Optimization Algorithm (WOA) with a reference point defined

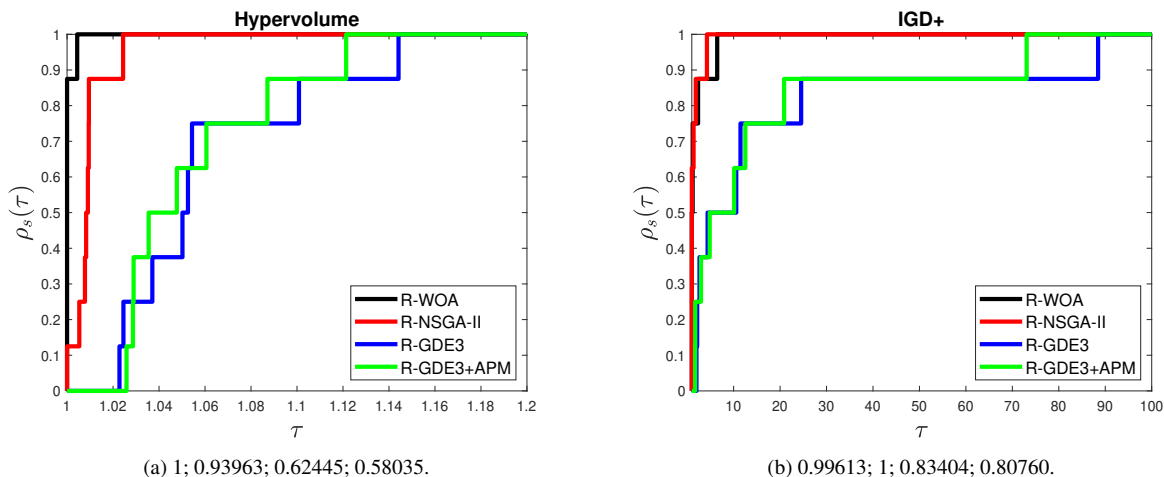


Figure 1. Performance profile curves relative to Hypervolumes (1a) and IGD+ (1b) values presented in Table 1. The areas under the curves (proportionally to the biggest) are displayed in the caption in the following order: R-WOA; R-NSGA-II; R-GDE3+APM; R-GDE3.

as DM's aspiration values of the objective functions. This algorithm was used to solve the continuous cases of MOSOPs containing 10-, 25-, 60-, 72-, and 942-bar trusses, also considering discrete cases for some of them. The obtained results were compared with other algorithms in the literature (R-NSGA-II, R-GDE3, and R-GDE3+APM) regarding Hypervolume and IGD+ performance measures. The non-parametric Wilcoxon Rank Sum statistical test and Performance Profiles were used to provide an in-depth analysis of the Hypervolume and IGD+ results.

The experiments showed that R-WOA achieved the best performance regarding the Hypervolume indicator, attaining the best mean for almost all problems with statistically significant differences in most cases. Furthermore, R-WOA reached the second-best performance concerning IGD+, getting competitive results compared to the MOEA with the best IGD+ performance (R-NSGA-II). It was argued that R-WOA pointed out here is able to obtain a better distributed Pareto front in the ROI for some MOSOPs, compared to the other MOEAs. Also, R-WOA generated Pareto optimal solutions closer to the reference point than those achieved by the other considered algorithms in the 60-bar truss MOSOP (continuous case).

For future work, R-WOA needs to be used to solve other MOSOPs and other real-world engineering multi-objective optimization problems. Furthermore, an integration between R-WOA and Differential Evolution or SBX can improve the algorithm performance when solving MOSOPs.

Acknowledgements. The authors thank FAPEMIG (TEC APQ 00408-21 and TEC PPM 174-18), CAPES, CNPq (grant 308105/2021-4), and Federal Center for Technological Education of Minas Gerais (CEFET-MG) for their support.

Authorship statement. The authors hereby confirm that they are the sole liable persons responsible for the authorship of this work, and that all material that has been herein included as part of the present paper is either the property (and authorship) of the authors, or has the permission of the owners to be included here.

References

- [1] A. C. C. Lemonge, J. P. G. Carvalho, P. H. Hallak, and D. E. C. Vargas. Multi-objective truss structural optimization considering natural frequencies of vibration and global stability. *Expert Systems With Applications*, vol. 155, pp. 113777, 2021.
- [2] D. E. Vargas, A. C. Lemonge, H. J. Barbosa, and H. S. Bernardino. Solving multi-objective structural optimization problems using gde3 and nsga-ii with reference points. *Engineering Structures*, vol. 239, pp. 112187, 2021.
- [3] S. Mirjalili and A. Lewis. The whale optimization algorithm. *Advances in Engineering Software*, vol. 95, pp. 51–67, 2016.

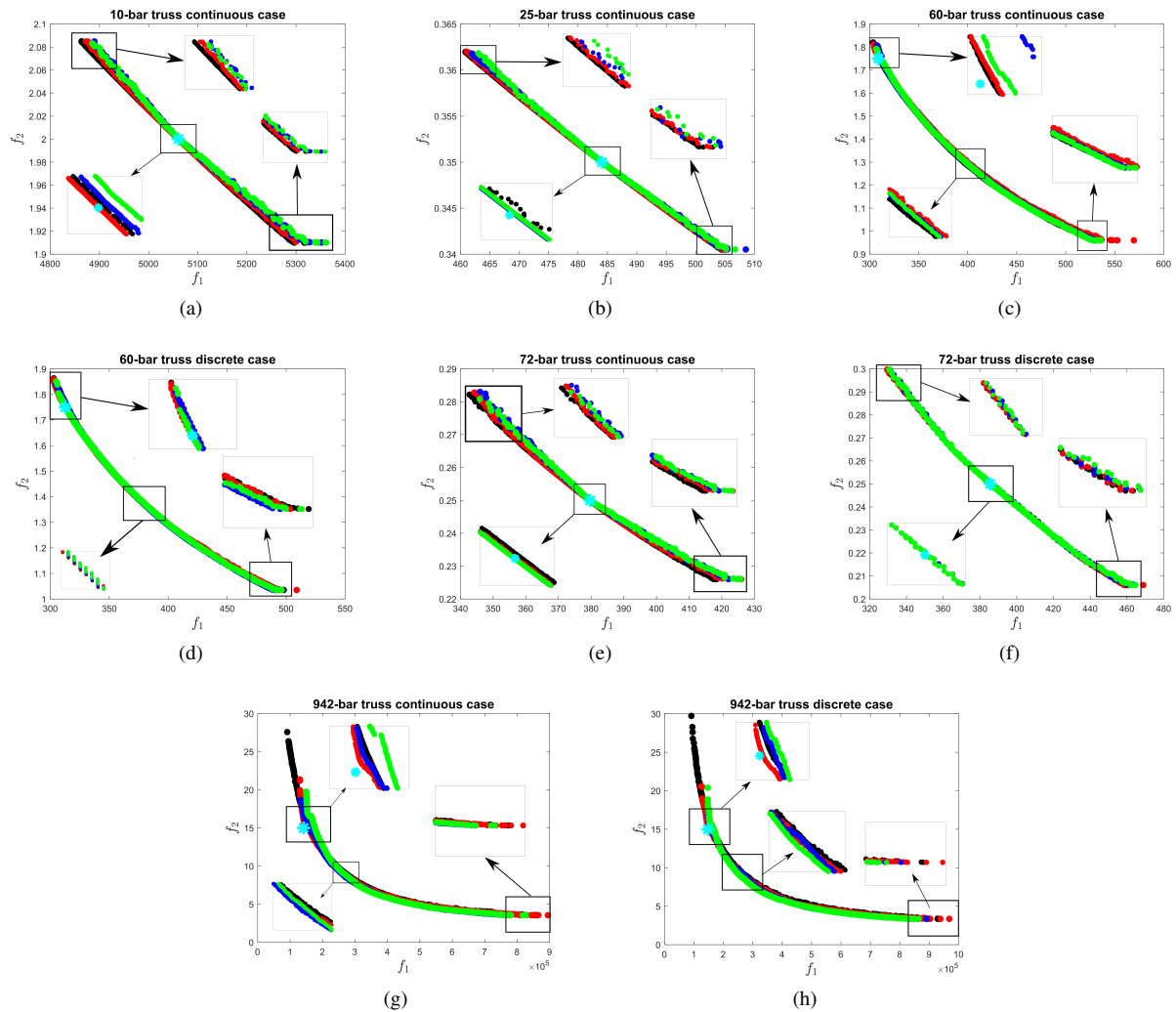


Figure 2. Combined Pareto front in DM's ROI enlarged in the middle and extremities of the Pareto front: R-WOA (black), R-NSGA-II (red), R-GDE3 (blue), and R-GDE3+APM (green). The reference point is in light blue.

- [4] K. Deb and J. Sundar. Reference point based multi-objective optimization using evolutionary algorithms. In *GECCO'06: Proc. of the Genetic and Evolutionary Computation Conference.*, pp. 635–642, New York, 2006.
- [5] K. Deb, A. Pratap, S. Agarwal, and T. Meyarivan. A fast and elitist multiobjective genetic algorithm: NSGA-II. *IEEE Trans. on Evolutionary Computation*, vol. 2(6), pp. 182–197, 2002.
- [6] D. E. C. Vargas, A. C. C. Lemonge, H. J. C. Barbosa, and H. S. Bernardino. Differential evolution with the adaptive penalty method for structural multi-objective optimization. *Optimization and Engineering*, vol. 20, pp. 65–88, 2019.
- [7] E. Zitzler and L. Thiele. Multiobjective evolutionary algorithms: A comparative case study and the strength Pareto approach. *IEEE Trans. on Evolutionary Computation*, vol. 3(4), pp. 257–271, 1999.
- [8] H. Ishibuchi, H. Masuda, Y. Tanigaki, and Y. Nojima. Modified distance calculation in generational distance and inverted generational distance. In *In: Gaspar-Cunha A., Henggeler Antunes C., Coello C. (eds) Evolutionary Multi-Criterion Optimization. EMO 2015. Lecture Notes in Computer Science, vol 9019.*, pp. 110–125. Springer, Cham., 2015.
- [9] E. D. Dolan and J. More. Benchmarking optimization software with performance profiles. *Mathematical Programming*, vol. 91, pp. 201–213, 2002.
- [10] H. J. C. Barbosa, H. S. Bernardino, and A. M. S. Barreto. Using performance profiles to analyze the results of the 2006 CEC constrained optimization competition. In *2010 IEEE World Congress on Computational Intelligence - WCCI*, pp. 1–8, 2010.